The Src and Abl family kinases activate the Spleen Tyrosine Kinase to maximize phagocytosis and *Leishmania* infection

Running title: *SYK mediates Leishmania infection*

Imran Ullah[1, 2, #], Umaru Barrie[1, 3], Rebecca M. Kernen[1,4], Emily T. Mamula[1], Arani Datta[1], Laela M. Booshehri[1,^], Emma L. Rhodes[1], James M. Bradford[1,+], and Dawn M. Wetzel[1, 2*]

[1]Department of Pediatrics, University of Texas Southwestern Medical Center, 5323 Harry Hines Blvd, Dallas, Texas, 75390, United States. [2]Department of Biochemistry, University of Texas Southwestern Medical Center, 5323 Harry Hines Blvd, Dallas, Texas, 75390, United States. [3]Medical Scientist Training Program, University of Texas Southwestern Medical Center, 5323 Harry Hines Blvd, Dallas, Texas, 75390, United States. [4]Emergency Medicine Residency Program, University of Texas Southwestern Medical Center, 5323 Harry Hines Blvd, Dallas, Texas, 75390, United States

*Corresponding author: Email: dawn.wetzel@utsouthwestern.edu

[#]Present Address: Department of Immunology and Infectious Diseases, Harvard T.H. Chan School of Public Health, Boston, MA 02115, USA

^Present Address: Doctoral Program, Scripps Institution of Oceanography, UC San Diego, La Jolla, CA, 92093

[+]Present Address: Dell Medical School, UT Austin, Austin, TX, 78712

Keywords: *Leishmania*, kinase, pathogen, parasite, macrophage

Abbreviations: BMDM, bone marrow-derived macrophages; CR3, complement receptor 3; FcR, Fc receptor; h, hour; Mϕ, macrophage; m, minutes; SE, standard error; p-, phosphorylated; SFK, Src family kinases; SYK, spleen tyrosine kinase

SUMMARY STATEMENT

Activation of Spleen Tyrosine Kinase by Src and Abl family kinases is required for maximal *Leishmania* uptake by macrophages and disease in a mouse model of cutaneous leishmaniasis.

ABSTRACT

Leishmania spp. are obligate intracellular parasites that must be internalized by phagocytic cells to evade immune responses and cause disease. *Leishmania* uptake is thought to be mainly host cell-driven, not parasite-driven. Promastigote (insect-stage) parasites primarily bind complement receptors (*e.g.*, CR3) on phagocytes and are internalized through a process analogous to complement-mediated phagocytosis. Amastigote-stage parasites (proliferative forms in humans and mice) primarily bind Fc receptors and are engulfed through a process similar to immunoglobulin-mediated phagocytosis. Our previous work indicates that host Src and Abl family kinases facilitate *Leishmania* entry into macrophages and pathogenesis in murine cutaneous leishmaniasis. Here we demonstrate that host spleen tyrosine kinase (SYK) is required for efficient uptake of *Leishmania* promastigotes and amastigotes. A Src family kinase-Abl family kinase-SYK signaling cascade induces *Leishmania* amastigote internalization. Finally, lesion size and parasite burden during *Leishmania* infection is significantly decreased in mice lacking SYK in monocytes or by treatment with the SYK inhibitor entospletinib. In summary, SYK is required for maximal *Leishmania* uptake by macrophages and disease in mice. Our results suggest potential for treating leishmaniasis using host cell-directed agents.

55 **INTRODUCTION**

56 Approximately 350 million people worldwide are at risk for the disfiguring
57 cutaneous or fatal visceral forms of leishmaniasis, which is a neglected tropical disease
58 (WHO, 2022). The drugs currently used to treat leishmaniasis have poor efficacy and/or
59 are highly toxic to human hosts; therefore, new antiparasitics are urgently needed (Wetzel
60 and Phillips, 2018). Leishmaniasis results from infection by obligate intracellular parasites
61 in the *Leishmania* genus. During its life cycle, *Leishmania* alternates between
62 promastigotes, found in sand fly vectors, and amastigotes, found in vertebrate hosts such
63 as humans, dogs and rodents. In order for infection to be established in humans after a
64 sand fly bite, phagocytic cells (*e.g.*, neutrophils, macrophages [Mϕ]) must ingest
65 promastigotes, using a process that is thought to be primarily driven by the host cell. The
66 parasites survive in acidic phagolysosomes, where they differentiate into amastigotes and
67 multiply. If amastigotes exit this compartment, they must be taken up again by phagocytes
68 to survive within their vertebrate hosts. *Leishmania* parasites that remain outside of
69 phagocytic cells are thought to either die or be killed by the host immune system.

70

71 Multiple protein receptors on the surfaces of phagocytic cells have been implicated
72 in the process of *Leishmania* uptake. For example, promastigotes bind the complement
73 receptor CR3; this process is enhanced when parasites are opsonized (coated) with the
74 terminal component of complement, C3bi (Mosser *et al.*, 1992; Puentes *et al.*, 1988;
75 Russell and Wright, 1988). Amastigotes are opsonized with immunoglobulin G (IgG) and
76 bind the Fc receptor subclass FcγR (Guy and Belosevic, 1993), which is required for a
77 productive *in vivo* infection (Kima *et al.*, 2000). After *Leishmania* binds cell surface

78 receptors, actin-rich phagocytic cups form and surround the parasites, allowing them to
79 be internalized (Lodge and Descoteaux, 2008). However, the host cell signaling process
80 that drives *Leishmania* uptake has not been well-described.
81
82 Previously, we implicated host Src family kinases (SFK) as well as Abl family
83 kinases in the process of *Leishmania amazonensis* uptake by Mϕs. The SFK, and
84 specifically Hck, Fgr, and Lyn, are non-receptor tyrosine kinases that had been known to
85 participate in IgG-mediated phagocytosis (Fitzer-Attas *et al.*, 2000) after pathogens bind
86 the Fc Receptor (FcR) (Wu *et al.*, 2001). Using SFK inhibitors such as SU6656 and
87 primary Mϕs lacking Hck, Fgr, and Lyn, we demonstrated that SFK were necessary for
88 maximal amastigote uptake by Mϕ, as well as for disease in a mouse model of cutaneous
89 leishmaniasis (Wetzel *et al.*, 2016). SFK bind and phosphorylate another set of non-
90 receptor tyrosine kinases, the Abl family kinases Abl (Abl1) and Arg (Abl2) (Mader *et al.*,
91 2011; Plattner *et al.*, 2004; Tanis *et al.*, 2003); (Bradley and Koleske, 2009). We have
92 shown that Abl and Arg facilitate complementary activities during phagocytosis and
93 *Leishmania* uptake by Mϕ (Wetzel *et al.*, 2012). Specifically, Mϕ isolated from mice lacking
94 Arg (*Arg-/-* Mϕ*)* exhibited reduced phagocytosis of IgG-coated beads or amastigotes, but
95 have no defects in the uptake of C3bi-coated beads or promastigotes (Wetzel *et al.*,
96 2012). Conversely, Mϕ from mice lacking Abl (*Abl-/-* Mϕ) show defects in the uptake of
97 C3bi-coated beads and promastigotes, but have no defects in the internalization of IgG-
98 coated beads or amastigotes (Wetzel *et al.*, 2012). Mϕ lacking both Abl family kinases
99 have no deficiencies in C3bi or IgG-mediated uptake beyond that seen for Mϕs lacking
100 the single relevant kinase (Wetzel *et al.*, 2012; Wetzel *et al.*, 2016). Mice lacking Abl or

101 Arg, or treated with the Abl family kinase inhibitor imatinib, had smaller lesions and lower
102 parasite burden in a cutaneous mouse model of leishmaniasis (Wetzel *et al.*, 2012).
103 Finally, treatment of *Leishmania*-infected mice with bosutinib, which inhibits both Abl
104 family kinases and SFK, led to greater decreases in lesion size and parasite burden than
105 were seen with inhibition of either kinase family alone (Wetzel *et al.*, 2016).
106
107 Spleen Tyrosine Kinase (SYK) is a cytoplasmic tyrosine kinase with 10 tyrosines
108 that can be phosphorylated to participate in signal transduction from immune receptors
109 such as FcR (Furlong *et al.*, 1997). Mϕ derived from mice conditionally lacking SYK in
110 immune cells are defective in several FcR-induced signaling events (Bonnerot *et al.*,
111 1998; Bradshaw, 2010; Lowell, 2011). These Mϕ also have deficits in IgG-mediated
112 phagocytosis; they form actin-rich phagocytic cups but cannot close them around
113 pathogens (Crowley *et al.*, 1997). However, Mϕ respond normally to lipopolysaccharide
114 (LPS), indicating that there are no deficiencies in activation (Crowley *et al.*, 1997). Some
115 laboratories have suggested that SYK inhibition does not affect C3bi-mediated
116 phagocytosis (Kiefer *et al.*, 1998), but others have shown significant defects in this
117 process (Tohyama and Yamamura, 2006; Walbaum *et al.*, 2021). There do not appear to
118 be SYK homologs in *Leishmania* (Baker *et al.*, 2021; Parsons *et al.*, 2005).
119
120 Prior studies suggest that kinases previously implicated in *Leishmania*
121 internalization also may modulate SYK-mediated processes in related biological systems.
122 For example, Mϕ derived from mice deficient for Hck, Fgr, and Lyn exhibited decreased
123 SYK activation when FcR was crosslinked by antibodies (Crowley *et al.*, 1997). In

124 addition, loss of Abl/Arg activity limited SYK phosphorylation after FcR crosslinking with
125 antibodies, and Arg kinase phosphorylated SYK in kinase assays with purified proteins
126 (Greuber and Pendergast, 2012). Based on these prior findings, we hypothesized that
127 host cell SYK would be activated by SFK and Abl family kinases during the uptake of
128 *Leishmania* by macrophages, and that SYK activity would be required for pathogenesis
129 in a mouse model of leishmaniasis.
130
131 Here, we demonstrate that host cell SYK facilitates both C3bi- and IgG-mediated
132 phagocytosis and promotes the internalization of *Leishmania* promastigotes and
133 amastigotes. A SFK-Abl family kinase-SYK pathway is required for maximal
134 internalization of *Leishmania* amastigotes by Mϕ. In addition, mice lacking SYK in
135 monocytes, as well as mice treated with the SYK kinase inhibitor entospletinib, have
136 significantly reduced lesion severity and parasite burden in a mouse model of cutaneous
137 *Leishmania* infection. Our results provide proof-of-concept that leishmaniasis could
138 potentially be treated with agents directed at host cell kinases such as SYK.

139 **RESULTS**

140 **Entospletinib decreases complement and immunoglobulin-mediated phagocytosis**

141 Previously, we have shown that SFK inhibitors and Abl family kinase inhibitors
142 decrease the uptake of *Leishmania* parasites (Wetzel *et al.*, 2012; Wetzel *et al.*, 2016).
143 Others have suggested that signaling during phagocytosis by these two kinase families
144 can be relayed to SYK (Crowley *et al.*, 1997; Greuber and Pendergast, 2012). Therefore,
145 we chose to explore the role of SYK in phagocytic model systems and *Leishmania* uptake
146 by Mϕ. Entospletinib is a SYK inhibitor that has an IC_{50} of 7.7 nM in purified kinase assays
147 (Ramanathan *et al.*, 2017). Given its recent favorable results in a human phase 1b/2 trial
148 for acute myeloid leukemia (Walker *et al.*, 2020), it is an attractive tool for further study.
149 However, its effects on phagocytosis had not been documented previously. For this
150 reason, we first determined whether entospletinib treatment of phagocytic cells affected
151 immunoglobulin-mediated phagocytosis. We treated RAW 264.7 cells, a murine Mϕ-like
152 cell line, with increasing concentrations of entospletinib or DMSO for 2 hours (h) and
153 incubated them for 30 minutes (m) with beads that had been coated with IgG. We found
154 that entospletinib, in a concentration-dependent manner, decreased the uptake of IgG-
155 coated beads, as demonstrated by the phagocytic index or number of internalized beads
156 per 100 Mϕs (PI, Fig. S1A). Based on this titration, we selected a concentration of 1 μM
157 for further studies.

158

159 Whether SYK plays a role in C3bi-mediated phagocytosis has been a subject of
160 debate (Kiefer *et al.*, 1998; Tohyama and Yamamura, 2006; Walbaum *et al.*, 2021). To
161 determine whether entospletinib treatment of host cells affected C3bi and IgG-mediated

162 phagocytosis, we treated RAW 264.7 cells with 1 μM entospletinib or DMSO for 2 h and
163 incubated them for 30 m with beads that had been coated with C3bi or IgG. We found
164 that 1 μM entospletinib decreased both C3bi-coated and IgG-coated bead uptake by RAW
165 264.7 cells by 44 ± 6% and 67 ± 8% (mean ± standard error [SE]), respectively (Fig. 1A,
166 B). These results were confirmed with primary bone marrow-derived Mϕs (BMDM)
167 isolated from mouse tibias/femurs (Fig. 1C). The decreases in C3bi- and IgG-mediated
168 phagocytosis due to entospletinib treatment specifically resulted from defects in
169 internalization, as entospletinib did not affect the total (internal + external) number of C3bi-
170 and IgG-coated beads normalized to the number of RAW 264.7 cells (Fig. 1D) or BMDM
171 (Fig. 1E).
172

173 **SYK inhibition decreases *Leishmania* promastigote and amastigote uptake by Mϕs**

174 We can grow both promastigotes and amastigotes of *L. amazonensis* without
175 mammalian host cells (axenic cultures), using a supplemented growth media at pH 7.2
176 for promastigotes or pH 5 for amastigotes (Hodgkinson *et al.*, 1996). To test whether
177 entospletinib treatment also affected the internalization of promastigotes and axenic
178 amastigotes, we again pre-treated Mϕs with 1 μM entospletinib or DMSO, but now
179 incubated them with C3bi-coated *L. amazonensis* promastigotes or IgG-coated axenic
180 amastigotes. We found that 1 μM entospletinib decreased promastigote and amastigote
181 uptake by RAW 264.7 cells (by 39 ± 3% and 54 ± 5% respectively; Fig. 2A, B) and BMDM
182 (by 49 ± 6% and 66 ± 6%; Fig. 2C). Titration of entospletinib demonstrated that amastigote
183 uptake by RAW 264.7 cells was decreased in a concentration-dependent manner (Fig.
184 S1B). Entospletinib did not affect the total number of promastigotes or amastigotes that

185 bound RAW 264.7 cells (Fig. 2D) or BMDM (Fig. 2E). In addition, measuring uptake over
186 longer periods (up to 3 h) did not enable treated RAW 264.7 cells to overcome
187 entospletinib-mediated defects in *Leishmania* internalization (Fig. S1C).
188
189 To ensure that entospletinib did not have deleterious effects on *L. amazonensis*
190 amastigotes, we incubated axenic amastigotes with entospletinib for 72 h and assessed
191 parasite survival with alamarBlue® (Ullah *et al.*, 2020). Entospletinib's EC_{50} against
192 axenic amastigotes in this assay was > 20 μM. The CC_{50} for RAW 264.7 cells over 72 h
193 was 3.3 ± 1.2 μM (3 biological replicates performed; see representative log concentration
194 response curves in Fig S1D). These studies indicated that entospletinib did not kill either
195 *Leishmania* parasites or host cells over the time period and concentrations studied in
196 these uptake assays. To test whether entospletinib affected the intracellular survival of *L.*
197 *amazonensis* amastigotes post-internalization, we engineered *L. amazonensis* parasites
198 that expressed mNeonGreen (see methods) and allowed these amastigotes to be taken
199 up by RAW 264.7 cells. 24 h later, we added DMSO or 0.5 μM entospletinib (a
200 concentration where effects on host cells were minimal) for 72 h. We found no apparent
201 defects in the ability of amastigotes to survive within 0.5 μM entospletinib-treated RAW
202 264.7 cells compared to DMSO-treated RAW 264.7 cells over 72 h (Fig S1E).
203
204 **Host cell SYK is required for efficient phagocytosis and *Leishmania* uptake by Mϕs**
205 Given that kinase inhibitors can potentially have off-target effects, and could also
206 be acting upon either parasites or host cells, we next specifically tested the role of host
207 cell SYK during *Leishmania* uptake by Mϕs. Using BMDMs isolated from mice lacking

208 SYK in the monocyte lineage (*Syk*$^{flox/flox}$ LysM Cre+, abbreviated as *Syk*$^{-/-}$ when
209 discussing isolated BMDM), we found that *Syk*$^{-/-}$ BMDM demonstrated decreases in
210 promastigote (Fig. 3A, B) and amastigote uptake (Fig. 3B), by 38 ± 5% and 73 ± 3%,
211 respectively. The total number of promastigotes or amastigotes bound to BMDM was not
212 affected (Fig. 3C). *Syk*$^{-/-}$ BMDM also exhibited defects in C3bi and IgG-mediated
213 phagocytosis of coated beads (which were decreased by 43 ± 3% and 65 ± 10%,
214 respectively; Fig. 3D, E).
215

216 ***Leishmania* stimulates SFK-Arg-SYK signaling in Mϕs to stimulate uptake**

217 SFK and Abl family kinases have been shown to partly signal through SYK in
218 previous studies (Greuber and Pendergast, 2012). We have shown that Hck/Fgr/Lyn
219 specifically activates Abl2/Arg to facilitate amastigote uptake by Mϕs (Wetzel *et al.*, 2012;
220 Wetzel *et al.*, 2016). SFK are not required for C3bi-mediated phagocytosis in our system
221 (Wetzel *et al.*, 2016). Abl1, but not SFK or Arg, is required for efficient promastigote
222 uptake (Wetzel *et al.*, 2012; Wetzel *et al.*, 2016). Therefore, we hypothesized that an FcR-
223 SFK-Arg-SYK signaling pathway would be required for amastigote uptake, and a CR3-
224 Abl-SYK signaling pathway would be responsible for promastigote uptake. To test this
225 hypothesis, we performed experiments using combinations of kinase inhibitors and
226 activators (Mohamed *et al.*, 2022). Treating *Syk*$^{-/-}$ BMDM with imatinib to inhibit Abl family
227 kinases did not further decrease *Leishmania* promastigote uptake, and similarly, treating
228 *Syk*$^{-/-}$ BMDM with SU6656 to inhibit SFK or imatinib to inhibit Abl family kinases did not
229 further diminish *Leishmania* amastigote uptake (Fig. 4A). Adding entospletinib neither
230 further decreased promastigote uptake by BMDM lacking Abl (*Abl*$^{flox/flox}$ LysM Cre+

231 BMDM; abbreviated in figure as *Abl*$^{-/-}$) nor further impaired amastigote uptake by BMDM
232 lacking Hck, Fgr, and Lyn (*HFL*$^{-/-}$ BMDM) or Arg (*Arg*$^{-/-}$ BMDM) kinases (Fig. 4B). In
233 addition, the Arg/Abl activator DPH did not rescue the uptake of *Leishmania*
234 promastigotes or amastigotes by *Syk*$^{-/-}$ BMDM (Fig. 4C).
235
236 We then investigated whether SFK and Abl family kinases were essential for SYK
237 activation during amastigote uptake. We allowed Mϕs to begin internalizing amastigotes
238 and performed immunoblots for phosphorylated SYK (pSYK), normalized to total SYK
239 levels. We found that pSYK levels were decreased after inhibition of SFK (using SU6656)
240 or Abl family kinases (using imatinib), while activating Abl family kinases using DPH
241 increased Syk phosphorylation (Fig. 5A, B). Previously, we have shown that SFK and Abl
242 family kinases are required for effective phosphorylation of their substrate CrkII (*i.e.*, pCrk)
243 during amastigote uptake by Mϕs (Wetzel *et al.*, 2012; Wetzel *et al.*, 2016). To determine
244 whether SYK was required for this phosphorylation event, we probed for pCrk induction
245 upon amastigote uptake by entospletinib-treated Mϕs. We found lower levels of pCrk in
246 entospletinib-treated Mϕs undergoing amastigote uptake when compared to DMSO
247 controls (Fig. 5C, D).
248
249 **SYK inhibition reduces lesion size and parasite burden in cutaneous leishmaniasis**
250 Knowing that SYK was required for efficient uptake of *Leishmania* by Mϕs, we next
251 investigated whether its activity was required for the manifestations of cutaneous
252 leishmaniasis in mice. We infected *Syk*$^{flox/flox}$ LysM Cre+ mice and WT mice in the right
253 hind foot with *L. amazonensis* and monitored lesion size over time. We found that

254 *Syk*$^{flox/flox}$ LysM Cre+ mice developed smaller lesions than WT mice (Fig. 6A), suggesting
255 that SYK activity is necessary for maximal pathogenesis of cutaneous leishmaniasis in
256 the mouse model.
257
258 The smaller lesions seen in *Syk*$^{flox/flox}$ LysM Cre+ mice potentially could be the
259 result of differences in their immunological responses to infection. As a simplified
260 paradigm, Th1 responses to leishmaniasis are typically protective, and Th2 responses
261 are generally deleterious to the infected host (Jones *et al.*, 1998). Therefore, we isolated
262 draining lymph nodes from infected WT and *Syk*$^{flox/flox}$ LysM Cre+ mice and assayed
263 cytokine secretion after stimulation with parasite lysates. Overall, we found limited
264 differences between these two categories of mice (Table 1), with the exception of IL1β
265 induction, which SYK is known to facilitate (Callaway *et al.*, 2015). However, decreases
266 in IL1β have been associated with lesion worsening (Lima-Junior *et al.*, 2013). We also
267 did not see any changes in the overall ratio of Th1 vs Th2 cytokine release (Table S1).
268
269 Based on our data that SYK activity is required for *Leishmania* uptake by
270 macrophages, we hypothesized that there would be fewer parasites contained within
271 lesions of infected *Syk*$^{flox/flox}$ LysM Cre+ mice. Indeed, at experimental termination, we
272 found that lesions in *Syk*$^{flox/flox}$ LysM Cre+ mice contained fewer parasites than WT mice
273 (Fig. 6B).
274
275 Next, we tested whether inhibition of SYK with entospletinib decreased lesion size
276 and parasite burden. We found that entospletinib-treated mice developed smaller lesions

277 than untreated mice over time (Fig. 6C). There were minimal effects on cytokine secretion
278 when draining lymph nodes isolated from DMSO-treated infected mice were treated with
279 entospletinib during cell culture (Table 2). The lone statistically significant result was an
280 increase in IL-13 in some stimulated entospletinib-treated samples. Finally, we
281 demonstrated that lesions in entospletinib-treated mice contained significantly fewer
282 parasites than DMSO-treated mice (Fig. 6D).
283
284 In summary, we have demonstrated that SFK and Abl family kinases activate SYK
285 to facilitate phagocytosis, the uptake of *Leishmania* by Mϕs, and the disease
286 manifestations seen in experimental cutaneous leishmaniasis. In combination with our
287 previous results (Wetzel *et al.*, 2012; Wetzel *et al.*, 2016), these findings suggest that
288 preventing parasite uptake by host cells using kinase inhibitors could be a valid strategy
289 for designing novel antileishmanial therapies.
290

291 **DISCUSSION**

292 We have shown previously that host SFK and Abl family kinases promote
293 *Leishmania* uptake by Mϕs (Wetzel *et al.*, 2012; Wetzel *et al.*, 2016). Our results here
294 demonstrate that SYK also is necessary for maximal *Leishmania* promastigote and
295 amastigote uptake by Mϕs. Activation of SYK by SFK and Abl family kinases in Mϕs
296 facilitates *Leishmania* internalization. Finally, mice lacking SYK in monocytes or treated
297 with the SYK kinase inhibitor entospletinib exhibited significantly reduced lesion severity
298 and parasite burden when infected with *Leishmania amazonensis*. Our data lead us to
299 propose a relationship between FcR signaling, SFKs, Arg, and SYK during *Leishmania*
300 amastigote uptake (Fig. 6E). Upon FcR ligation by amastigotes, Hck, Fgr, and Lyn are
301 activated. These SFKs phosphorylate and activate Arg kinase, which phosphorylates and
302 activates SYK, which leads to activation of CrkII, actin polymerization at the site of cell
303 entry and formation/closure of the phagocytic cup (Fig. 6E).

304

305 Engagement of FcR stimulates downstream responses important for host
306 immunity and receptor-mediated phagocytosis. Our results demonstrate that FcR-
307 mediated signals permitting *Leishmania* amastigote uptake are relayed to SYK. SYK
308 previously was shown to facilitate phagocytosis after opsonized particles bind FcR on
309 phagocytic cells (Crowley *et al.*, 1997). Reductions in IgG-mediated phagocytosis by
310 *Syk*$^{-/-}$ BMDM are secondary to defects in phagocytic cup formation and closure, rather
311 than defects in Mϕ activation (Crowley *et al.*, 1997). The effects of the novel SYK inhibitor,
312 entospletinib, on phagocytosis had not been explored to date. We find that fewer IgG-
313 coated beads or *Leishmania* amastigotes are internalized by entospletinib-treated Mϕ or

314 Mϕ deficient in SYK. Neither condition changes the numbers of beads or parasites bound
315 to Mϕ. The role of SYK in C3bi-mediated phagocytosis has been somewhat controversial
316 (Kiefer *et al.*, 1998; Tohyama and Yamamura, 2006; Walbaum *et al.*, 2021). Our data add
317 to the evidence that SYK is necessary for efficient C3bi-mediated phagocytosis.
318 Importantly, we also establish that SYK promotes the uptake of *Leishmania*
319 promastigotes.
320
321 In combination with previous studies, our experiments indicate that the specific
322 signaling events necessary for FcR-mediated *Leishmania* amastigote internalization are
323 initiated by the activation of SFK, which proceed to phosphorylate Arg kinase, which in
324 turn phosphorylates SYK. The pSYK antibody used here specifically recognizes
325 phosphorylation on Tyr525/526, which are SYK autophosphorylation sites that are
326 necessary for maximal activity. Based on our data, we presume that Abl family kinases
327 are modulating the phosphorylation of these two residues during amastigote uptake.
328 However, our data do not rule out the possibility that other sites on SYK may also be
329 phosphorylated. The link between Abl family kinases and SYK is likely to be direct, as
330 previous studies have demonstrated that purified Arg kinase phosphorylates SYK *in vitro*
331 (Bonnerot *et al.*, 1998; Greuber and Pendergast, 2012; Parsa *et al.*, 2008). Similarly, SFK
332 have been shown to phosphorylate Arg kinase *in vitro* (Mader *et al.*, 2011; Plattner *et al.*,
333 2004; Tanis *et al.*, 2003). In addition, this study, in combination with our prior work (Wetzel
334 *et al.*, 2012; Wetzel *et al.*, 2016) demonstrates that activation of SFK, Abl family kinases
335 and SYK after FcR binding results in CrkII activation during the uptake of *Leishmania*
336 parasites. A number of other downstream mediators of SYK signaling have been

337 published (Mocsai *et al.*, 2010). Our future studies will directly test whether these
338 mediators, or other kinases previously thought to facilitate phagocytosis or internalization
339 of other pathogens, also participate in the uptake of *Leishmania*.
340
341 Because *Leishmania* parasites that remain extracellular within a mammalian host
342 should either die or be killed by the host immune system, we tested whether SYK
343 deficiency would restrict disease manifestations in a mouse model of cutaneous
344 leishmaniasis. Our studies indicate that *Leishmania* survival and pathogenesis in mice
345 depends on SFK (Wetzel *et al.*, 2016), Abl/Arg (Wetzel *et al.*, 2012; Wetzel *et al.*, 2016),
346 and now SYK. We believe that the smaller lesions seen in SYK-deficient mice primarily
347 occur due to the deficits we identified in parasite internalization by phagocytes. Consistent
348 with this hypothesis, there are fewer parasites within the lesions of SYK-deficient mice or
349 mice treated with entospletinib. Since our hypothesis is difficult to test directly, our
350 conclusions in part stem from eliminating other possibilities. For example, we found that
351 entospletinib did not kill *Leishmania* parasites directly, and we saw no defects in parasite
352 survival within entospletinib-treated Mϕs.
353
354 Furthermore, we assessed whether the reductions in lesion size observed in SYK-
355 deficient mice could be due to variations in the host immune response to leishmaniasis
356 compared to control mice. For example, SYK deficiency is known to affect B and T cell
357 development in mice and immune cell adhesion (Mocsai *et al.*, 2010), which might would
358 adversely affect the host's ability to control infections. However, our results suggest that
359 such defects play a more limited role in our experimental system. The overall innate

360 immune response to leishmaniasis is complex and dependent upon the infecting parasite
361 species and the mouse strain used. In general, Th1 responses lead to lesion healing and
362 Th2 responses result in lesion worsening (Jones *et al.*, 1998). Our profiling of cytokines
363 secreted by isolated lymph nodes after infection revealed no significant differences in Th1
364 versus Th2 responses between SYK-deficient and control mice. Lymph nodes from
365 *Syk*$^{-/-}$ mice did exhibit defects in IL1-β secretion, which is known to be partly dependent
366 on SYK (Callaway *et al.*, 2015). However, we would expect that a decrease in IL1-β would
367 worsen lesions based on prior studies (Lima-Junior *et al.*, 2013). Similarly, we did not see
368 differences in secretion of cytokines from lymph nodes isolated from infected mice that
369 were incubated in entospletinib, save for an increase in IL-13 in some stimulated
370 entospletinib-treated samples, which also should not mediate lesion healing (Jones *et al.*,
371 1998). Therefore, we saw no differences in the immune response to leishmaniasis from
372 our cytokine profiling that would explain the decreased lesion size in mice deficient in
373 SYK or treated with entospletinib.
374

375 **CONCLUSION**

376 In summary, our studies demonstrate that SYK is required for maximal *Leishmania*
377 uptake by Mϕs and disease in mice. Our future work will continue to trace the signaling
378 pathways necessary for internalization of this parasite by Mϕ, with an eye towards using
379 inhibitors of these pathways as treatment for leishmaniasis. A host-targeted therapeutic
380 strategy is likely to be less susceptible to the development of resistance. While our studies
381 have thus far focused on *Leishmania*, our findings likely are more broadly applicable, as
382 other intracellular pathogens also utilize and activate SYK to facilitate receptor-mediated

383 uptake. For example, overexpression of membrane-targeted SYK in cells treated with Abl
384 kinase inhibitors partially rescues the impairment in phagocytosis of *Francisella tularensis*
385 (Parsa *et al.*, 2008). Thus, there is potential to harness host kinases such as SYK as
386 targets for a broad-spectrum antimicrobial agent against intracellular pathogens.
387

388 **MATERIALS AND METHODS**

389 **Mice**

390 The UT Southwestern Institutional Animal Care and Use Committee approved all animal
391 protocols. *Syk*$^{flox/flox}$ *LysM Cre*+ and *Syk*$^{flox/flox}$ *LysM Cre*- littermates were generated by
392 crossing *LysM Cre*+ mice to *Syk*$^{flox/+}$ mice (all on a C57BL/6J background, which along
393 with WT C57BL/6J mice, had been purchased from Jackson Labs (Bar Harbor, ME)).
394 *Hck*$^{-/-}$ *Fgr*$^{-/-}$ *Lyn*$^{-/-}$, *Arg*$^{-/-}$, *Abl*$^{flox/flox}$ *LysM Cre*+, and *Arg*$^{-/-}$ *Abl*$^{flox/flox}$ *LysM Cre*+ mice were
395 generated as described previously (Wetzel *et al.*, 2012). For all experiments, WT
396 littermates were paired with the kinase mutant under study to limit any effects from
397 variation in genetic backgrounds.

398

399 **Mammalian cell culture**

400 RAW 264.7 cells (obtained from ATCC, Manassas, VA) were incubated in Dulbecco's
401 modified Eagle's medium (DMEM) (ThermoFisher, Waltham, MA) plus 10% heat-
402 inactivated fetal bovine serum (FBS, Gemini). Bone marrow-derived primary Mϕs
403 (BMDM) were harvested from tibias of *Syk*$^{flox/flox}$ *LysM Cre*+, *Syk*$^{flox/flox}$ *LysM Cre*-, *Hck*$^{-/-}$
404 *Fgr*$^{-/-}$ *Lyn*$^{-/-}$, *Arg*$^{-/-}$, *Abl*$^{flox/flox}$ *LysM Cre*+, and/or *Arg*$^{-/-}$ *Abl*$^{flox/flox}$ *LysM Cre*+ mice and
405 confirmed as described (Wetzel *et al.*, 2012). All cells were screened for *Mycoplasma*
406 contamination (Wetzel *et al.*, 2016).

407

408 ***Leishmania* culture**

409 *L. amazonensis* strain IFLA/BR/67/PH8 promastigotes (obtained from Norma W.
410 Andrews, University of Maryland, College Park, MD) were grown in Schneider's

411 Drosophila medium (Sigma, St. Louis, MO) with 15% heat-inactivated FBS and 10 μg/ml
412 gentamicin (Sigma) (Wetzel *et al.*, 2012). 7 day old cultures were used for uptake
413 experiments to maximize yield of infective metacyclic promastigotes. *L. amazonensis*
414 strain IFLA/BR/67/PH8 amastigotes were grown axenically (outside of mammalian cells)
415 in supplemented Schneider's media at pH 5 as described (Hodgkinson *et al.*, 1996). All
416 parasites were serially passaged through mice so that virulence would be maintained.
417

418 **Transgenic *Leishmania* strains**

419 For intracellular survival assays, *L. amazonensis* expressing a bright monomeric
420 green fluorescent protein, mNeonGreen, was used. mNeonGreen was cloned into the
421 pLEXSY.hyg2 (Jenabioscience, Jena, Germany) expression vector with a hygromycin
422 resistance marker, as previously described (Ullah *et al.*, 2020). pLEXSY.hyg2 containing
423 mNeonGreen gene (pLEXSY.hyg2-mNeonGreen) was transfected into *L.*
424 *amazonensis* promastigotes using the Human T-Cell Nucleofector kit and the Amaxa
425 Nucleofector electroporator (program U-033, Lonza, Basel, Switzerland), for integration
426 into the 18S rRNA locus within the nuclear DNA. Following transfections, promastigotes
427 were allowed to grow for 24 h at 26 °C, then selected with 100 µg/mL hygromycin in
428 Schneider's Drosophila medium. Clones were isolated via limiting dilutions, and the
429 cultures were subsequently maintained in Schneider's Drosophila medium supplemented
430 with 100 µg/mL hygromycin. To maintain virulence, *L. amazonensis*-mNeonGreen
431 expressing parasites were passaged regularly in C57BL/6 mice, as described previously
432 (Wetzel *et al.*, 2016).
433

434 **Phagocytosis assays**

435 BMDM and RAW 264.7 cells were plated at > 50% confluence and starved overnight in
436 macrophage-colony stimulating factor (M-CSF)-starved or serum-free media. For drug
437 experiments, except where indicated, compounds were obtained from LC Laboratories
438 (Woburn, MA). Mϕ were incubated in 3.3 μM imatinib, 1 μM SU6656, 1 μM entospletinib,
439 or 0.1% DMSO (Sigma) for 2 h. For C3bi-coated bead internalization only, Mϕ were also
440 pre-activated with PMA (Sigma) for 1 h. As described (Wetzel *et al.*, 2012; Wetzel *et al.*,
441 2016), 2 μm latex green beads were incubated with human IgM (I-8260, Sigma), then in
442 rabbit anti-human IgM (Sigma 270A, IgG-coated beads) or fresh mouse serum (C3bi-
443 coated beads). 10 beads/ Mϕ were added to Mϕ for 30 m at 37 °C. To distinguish internal
444 from external beads, samples were fixed in 3% formaldehyde for 15 m, blocked in 2%
445 BSA (no permeabilization) (Wetzel *et al.*, 2004; Wetzel *et al.*, 2003; Wetzel *et al.*, 2005),
446 incubated in rabbit-anti human IgM and Hoescht 33258 (Sigma), and then incubated in
447 Alexa-Fluor-564-conjugated goat anti-rabbit IgG. Samples were visualized using a
448 Cytation 5 imager (BioTek, Santa Clara, CA) and analyzed by an observer blinded to
449 condition. Representative images for beads were collected on the Cytation 5 at 40X and
450 processed linearly in Adobe Photoshop (version 13.0.6) (Ullah *et al.*, 2020). The
451 phagocytic index (PI) was calculated as the number of beads internalized per 100 Mϕ,
452 and experimental samples were normalized to controls. The total number of beads per
453 100 Mϕ was also calculated, with experimental samples were normalized to controls. At
454 least 100 Mϕ and 100 beads were counted from multiple imaged fields per condition. 3
455 biological replicates were performed and means ± SE were calculated. Statistical
456 significance was determined by Student *t*-test or two-way ANOVA.

457

458 ***Leishmania* uptake assays**

459 RAW 264.7 cells or BMDMs were treated with DMSO/PMA/inhibitors as above. To allow
460 C3bi opsonization, we incubated metacyclic promastigotes in murine serum for 1 h. To
461 allow IgG opsonization, we intubated amastigotes with anti-P8 primary IgG1 antibody
462 (Pan and McMahon-Pratt, 1988) for 1 h. Opsonized parasites were incubated with Mϕ at
463 10:1 promastigotes per Mϕ or 2:1 amastigotes per Mϕ (Wetzel *et al.*, 2012; Wetzel *et al.*,
464 2016). Samples were fixed with 3% formaldehyde, blocked in 2% BSA in PBS, incubated
465 in mouse anti-gp46 antibody (promastigotes) or mouse anti-P8 antibody (both supplied
466 by Diane McMahon-Pratt), then incubated in Alexa-Fluor-568 goat-anti-mouse secondary
467 antibody (A10037, ThermoFisher) (Wetzel *et al.*, 2012). After permeabilization, parasites
468 were incubated in their original primary antibody, then Alexa-Fluor-488 donkey anti-
469 mouse secondary antibody (A21202, ThermoFisher) and Hoescht 33258 (Sigma).
470 Visualization, analysis, and statistics were performed as described above for bead
471 phagocytic assays (Wetzel *et al.*, 2012; Wetzel *et al.*, 2016). Representative images for
472 parasites were collected on a Zeiss LSM 880 inverted confocal Airyscan microscope at
473 40X (Ullah *et al.*, 2020). Shown are maximal intensity projections constructed from full Z-
474 thickness stacks through parasites/Mϕ using Image J (1.52a, http://imagej.nih.gov/ij) and
475 processed linearly in Adobe Photoshop (version 13.0.6) (Ullah *et al.*, 2020).

476

477 **Viability assays**

478 *L. amazonensis* promastigotes, axenic amastigotes, and RAW 264.7 cells were cultured
479 as above, added to 96 well plates containing dilution series of relevant compounds, and

480 incubated for 72 h before measuring viability using alamarBlue® (10%, ThermoFisher)
481 (Ullah *et al.*, 2020). Plates were read at 6 h with a BioTek Synergy H1 plate reader (530
482 nm excitation, 570 nm emission) (Ullah *et al.*, 2020). To assess for parasite survival, 10
483 *L. amazonensis* promastigotes/Mϕ were added to G-CSF starved WT BMDMs and
484 incubated for 4 h. After 5 washes with PBS, DMSO or 1 μm entospletinib was added in
485 media with G-CSF. Samples were analyzed after 72 h by microscopy using the Cytation
486 5 imager, and total numbers of amastigotes/Mϕ were calculated by a blinded observer
487 using the methods described above for phagocytosis assays.
488
489 **Immunoblotting**
490 To measure phosphorylation of SYK or CrkII, RAW 264.7 cells were incubated overnight
491 in serum-free media with experiments performed at ~70% confluence. To initiate
492 experiments, RAW cells were pre-incubated in 3.3 μM SU6656, 3.3 μM imatinib, 1 μM
493 entospletinib, 50 nM DPH or DMSO for 2 h. IgG-opsonized amastigotes were added to
494 adherent starved RAW 264.7 cells (at a ratio of 20:1) for 30 m (Pan and McMahon-Pratt,
495 1988). Cells were lysed with Pierce Radioimmunoprecipitation (RIPA) buffer (cat. no.
496 89901, Thermo Scientific, Rockford, IL) with protease and phosphatase inhibitors, and
497 protein concentrations were assessed using bicinchoninic acid (BCA) (cat. no. 23225,
498 Thermo Scientific). For representative images, equivalent protein amounts were loaded
499 on 10% SDS-PAGE gels, transferred to nitrocellulose membranes, and probed with
500 antibodies against phosphorylated Syk (pSyk) (Tyr525/526, cat. no. 2710S, Cell
501 Signaling, Danvers, MA) at 1:500, or Syk (cat. no. 2712S, Cell Signaling) at 1:500.
502 Immunoblotting with rabbit GAPDH (cat. no. 2118L, Cell Signaling) at 1:1000 was used

503 as a loading control. For analysis, relative amounts of pSyk or pCrkII were compared with
504 Image J analysis software and were normalized to Syk or CrkII (membranes were stripped
505 of pSyk or pCrk and reprobed for Syk or Crk). Imaging was performed by using a
506 phosphorimager (ImageQuant LAS 4000, GE, Boston, MA). Each experiment was
507 performed 3 times. Two-way ANOVA was used to determine statistical significance.
508

509 **Murine infections**

510 8 week old female C57BL/6 mice were infected in the dorsal side of the right hind foot
511 with 1 X 10^6 metacyclic promastigotes (isolated via Percoll gradient, Sigma) per mouse;
512 10 mice were used per experimental condition. All animals surviving until termination were
513 included in analysis. For entospletinib-treated mice, 3 experiments were conducted. Mice
514 were provided 100 mg/kg/d of entospletinib or the diluent (0.1 % DMSO) in their drinking
515 water at pH 5.5, starting 4 days prior to the experiment and continuing through termination
516 (Wetzel *et al.*, 2016). For *Syk*$^{flox/flox}$ *LysM Cre*+ mice, 3 independent experiments were
517 conducted. Lesion size was measured every other week with calipers by a condition-
518 blinded investigator, and infected/uninfected foot thickness ratios were calculated and
519 compared to time of infection by ANOVA. The number of parasites in lesions were
520 determined at the time of experiment termination (between 16 and 20 weeks post-
521 infection) (Soong *et al.*, 1997).

522 Lymph nodes from infected mice were harvested for cytokine profiling as described
523 (Wetzel *et al.*, 2012; Wetzel *et al.*, 2016). In brief, cells from lymph nodes were plated and
524 stimulated with varying concentrations of promastigote lysates or concanamycin A (CON
525 A) (5 μg/ml, Sigma); supernatants were harvested at 72 h. Levels of IL-1β, IL-4, IFN-γ, IL-

526 10, IL-13, and IL-17 were assessed by ELISA and compared to background
527 (unstimulated) levels.
528

529 **Acknowledgements**

530 We thank the parasitology group at UT Southwestern (Drs. James J. Collins, Margaret A.
531 Phillips, and Michael L. Reese), as well as members of the UT Southwestern
532 Departments of Biochemistry, Microbiology, Pharmacology, and Pediatrics, for valuable
533 discussions and use of common equipment. Gina M. Aloisio, Lauren T. Callaghan, Ivan
534 Luu, and T. Michael Oladugba provided expert technical assistance. Dr. Naomi S.
535 Morrissette (UC Irvine) supplied helpful comments on the manuscript, and Drs. Anthony
536 J. Koleske and Diane McMahon-Pratt (both from Yale University) offered valuable advice
537 as this project was conceived. Antileishmanial antibodies were donated by Dr. McMahon-
538 Pratt. *Arg*$^{-/-}$, *Abl*$^{flox/flox}$, and *Arg*$^{-/-}$ *Abl*$^{flox/flox}$ mice were provided by Dr. Koleske. *Hck*$^{-/-}$ *Fgr*$^{-/-}$
539 *Lyn*$^{-/-}$ mice were provided by Shaoguang Li. Confocal microscopy was performed in the
540 UT Southwestern Live Cell Imaging Facility.
541

542 **Competing interests**

543 The authors declare that they have no competing financial interests.
544

545 **Author contributions**

546 I.U., U.B., A.D., and D.M.W. designed and performed experiments, analyzed data, and
547 wrote the manuscript. R.M.K., E.T.M., L.M.B, E.L.R., and J.M.B. performed experiments
548 and analyzed data.

Funding

This work was supported by the National Institutes of Health (K08 AI103036 and R01 AI146349), a Children's Clinical Research Advisory Committee (CCRAC) Junior Investigator Award, a CCRAC Early Investigator Award, grant I-2086 from the Welch Foundation, and funds from the UT Southwestern Department of Pediatrics (all to D.M.W.). In addition, U.B. was supported by a National Institutes of Health Supplement To Promote Diversity in Health-Related Research (R01 AI146349-S1).

558 **REFERENCES**

559 Baker, N. *et al.* Systematic functional analysis of *Leishmania* protein kinases
560 identifies regulators of differentiation or survival. *Nat Commun*, **2021,** 12:1244.
561 Bonnerot, C. *et al.* Syk protein tyrosine kinase regulates Fc receptor gamma-
562 chain-mediated transport to lysosomes. *EMBO J*, **1998,** 17:4606-16.
563 Bradley, W. D. and Koleske, A. J. Regulation of cell migration and
564 morphogenesis by Abl-family kinases: emerging mechanisms and physiological
565 contexts. *J Cell Sci*, **2009,** 122:3441-54.
566 Bradshaw, J. M. The Src, Syk, and Tec family kinases: distinct types of molecular
567 switches. *Cell Signal*, **2010,** 22:1175-84.
568 Callaway, J. B. *et al.* Spleen Tyrosine Kinase (Syk) Mediates IL-1beta Induction
569 by Primary Human Monocytes during Antibody-enhanced Dengue Virus Infection. *J Biol*
570 *Chem*, **2015,** 290:17306-20.
571 Crowley, M. T. *et al.* A critical role for Syk in signal transduction and
572 phagocytosis mediated by Fcgamma receptors on macrophages. *J Exp Med*, **1997,**
573 186:1027-39.
574 Fitzer-Attas, C. J. *et al.* Fcgamma receptor-mediated phagocytosis in
575 macrophages lacking the Src family tyrosine kinases Hck, Fgr, and Lyn. *J Exp Med*,
576 **2000,** 191:669-82.
577 Furlong, M. T. *et al.* Identification of the major sites of autophosphorylation of the
578 murine protein-tyrosine kinase Syk. *Biochim Biophys Acta*, **1997,** 1355:177-90.
579 Greuber, E. K. and Pendergast, A. M. Abl family kinases regulate FcgammaR-
580 mediated phagocytosis in murine macrophages. *J Immunol*, **2012,** 189:5382-92.
581 Guy, R. A. and Belosevic, M. Comparison of receptors required for entry of
582 *Leishmania major* amastigotes into macrophages. *Infect Immun*, **1993,** 61:1553-8.
583 Hodgkinson, V. H. *et al. Leishmania amazonensis*: cultivation and
584 characterization of axenic amastigote-like organisms. *Exp Parasitol*, **1996,** 83:94-105.
585 Jones, D. E. *et al.* Host susceptibility factors to cutaneous leishmaniasis. *Front*
586 *Biosci*, **1998,** 3:D1171-80.
587 Kiefer, F. *et al.* The Syk protein tyrosine kinase is essential for Fcgamma
588 receptor signaling in macrophages and neutrophils. *Mol Cell Biol*, **1998,** 18:4209-20.
589 Kima, P. E. *et al.* Internalization of *Leishmania mexicana* complex amastigotes
590 via the Fc receptor is required to sustain infection in murine cutaneous leishmaniasis. *J*
591 *Exp Med*, **2000,** 191:1063-8.
592 Lima-Junior, D. S. *et al.* Inflammasome-derived IL-1beta production induces nitric
593 oxide-mediated resistance to Leishmania. *Nat Med*, **2013,** 19:909-15.
594 Lodge, R. and Descoteaux, A. *Leishmania* invasion and phagosome biogenesis.
595 *Subcell Biochem*, **2008,** 47:174-81.
596 Lowell, C. A. Src-family and Syk kinases in activating and inhibitory pathways in
597 innate immune cells: signaling cross talk. *Cold Spring Harb Perspect Biol*, **2011,** 3.
598 Mader, C. C. *et al.* An EGFR-Src-Arg-cortactin pathway mediates functional
599 maturation of invadopodia and breast cancer cell invasion. *Cancer Res*, **2011,** 71:1730-
600 41.
601 Mocsai, A. *et al.* The SYK tyrosine kinase: a crucial player in diverse biological
602 functions. *Nat Rev Immunol*, **2010,** 10:387-402.

603 Mohamed, M. F. *et al.* CrkII/Abl phosphorylation cascade is critical for NLRC4
604 inflammasome activity and is blocked by *Pseudomonas aeruginosa* ExoT. *Nat*
605 *Commun*, **2022,** 13:1295.
606 Mosser, D. M. *et al. Leishmania* promastigotes require opsonic complement to
607 bind to the human leukocyte integrin Mac-1 (CD11b/CD18). *J Cell Biol*, **1992,** 116:511-
608 20.
609 Pan, A. A. and McMahon-Pratt, D. Monoclonal antibodies specific for the
610 amastigote stage of *Leishmania pifanoi*. I. Characterization of antigens associated with
611 stage- and species-specific determinants. *J Immunol*, **1988,** 140:2406-14.
612 Parsa, K. V. *et al.* The tyrosine kinase Syk promotes phagocytosis of *Francisella*
613 through the activation of Erk. *Mol Immunol*, **2008,** 45:3012-21.
614 Parsons, M. *et al.* Comparative analysis of the kinomes of three pathogenic
615 trypanosomatids: *Leishmania major*, *Trypanosoma brucei* and *Trypanosoma cruzi*. *BMC*
616 *Genomics*, **2005,** 6:127.
617 Plattner, R. *et al.* Bidirectional signaling links the Abelson kinases to the platelet-
618 derived growth factor receptor. *Mol Cell Biol*, **2004,** 24:2573-83.
619 Puentes, S. M. *et al.* Complement binding by two developmental stages of
620 *Leishmania major* promastigotes varying in expression of a surface lipophosphoglycan.
621 *J Exp Med*, **1988,** 167:887-902.
622 Ramanathan, S. *et al.* Pharmacokinetics, Pharmacodynamics, and Safety of
623 Entospletinib, a Novel pSYK Inhibitor, Following Single and Multiple Oral Dosing in
624 Healthy Volunteers. *Clin Drug Investig*, **2017,** 37:195-205.
625 Russell, D. G. and Wright, S. D. Complement receptor type 3 (CR3) binds to an
626 Arg-Gly-Asp-containing region of the major surface glycoprotein, gp63, of *Leishmania*
627 promastigotes. *J Exp Med*, **1988,** 168:279-92.
628 Soong, L. *et al.* Role of CD4+ T cells in pathogenesis associated with *Leishmania*
629 *amazonensis* infection. *J Immunol*, **1997,** 158:5374-83.
630 Tanis, K. Q. *et al.* Two distinct phosphorylation pathways have additive effects on
631 Abl family kinase activation. *Mol Cell Biol*, **2003,** 23:3884-96.
632 Tohyama, Y. and Yamamura, H. Complement-mediated phagocytosis--the role of
633 Syk. *IUBMB Life*, **2006,** 58:304-8.
634 Ullah, I. *et al.* An antiparasitic compound from the Medicines for Malaria Venture
635 Pathogen Box promotes *Leishmania* tubulin polymerization. *ACS Infect Dis*, **2020,**
636 6:2057-2072.
637 Walbaum, S. *et al.* Complement receptor 3 mediates both sinking phagocytosis
638 and phagocytic cup formation via distinct mechanisms. *J Biol Chem*, **2021,** 296:100256.
639 Walker, A. R. *et al.* Entospletinib in combination with induction chemotherapy in
640 previously untreated Acute Myeloid Leukemia: response and predictive significance of
641 HOXA9 and MEIS1 Expression. *Clin Cancer Res*, **2020,** 26:5852-5859.
642 Wetzel, D. M. *et al.* Calcium-mediated protein secretion potentiates motility in
643 *Toxoplasma gondii*. *J Cell Sci*, **2004,** 117:5739-48.
644 Wetzel, D. M. *et al.* Actin filament polymerization regulates gliding motility by
645 apicomplexan parasites. *Mol Biol Cell*, **2003,** 14:396-406.
646 Wetzel, D. M. *et al.* The Abl and Arg kinases mediate distinct modes of
647 phagocytosis and are required for maximal *Leishmania* infection. *Molecular Cell*
648 *Biology*, **2012,** 32:3176-86.

649 Wetzel, D. M. and Phillips, M. A. Chapter 54: Chemotherapy of protozoal
650 infections. In *Goodman and Gilman's The Pharmacological Basis of Therapeutics*, (ed.
651 L. Brunton), New York, NY: McGraw-Hill Medical, 2018, pp. 987-999.
652 Wetzel, D. M. *et al.* The Src kinases Hck, Fgr, and Lyn activate Abl2/Arg to
653 facilitate IgG-mediated phagocytosis and *Leishmania* infection. *J Cell Sci*, **2016,**
654 129:3130-43.
655 Wetzel, D. M. *et al.* Gliding motility leads to active cellular invasion by
656 *Cryptosporidium parvum* sporozoites. *Infect Immun*, **2005,** 73:5379-87.
657 Wu, Y. *et al.* Role of Fc receptor gamma-chain in platelet glycoprotein Ib-
658 mediated signaling. *Blood*, **2001,** 97:3836-45.
659

660

661 **FIGURE LEGENDS**

662 **Fig. 1. The SYK inhibitor entospletinib decreases C3bi and IgG-mediated**
663 **phagocytosis**. Mϕs were treated with 1 μM entospletinib or DMSO for 2 h and incubated
664 with C3bi or IgG-coated beads for 30 m. A multi-colored immunofluorescence assay was
665 used to distinguish between extracellular (red) and intracellular (green) beads (see
666 methods for details). Nuclei are labeled with Hoescht 33258. (A) Image of anti-P8 C3bi-
667 opsonized bead uptake by RAW 264.7 cells treated with DMSO (top) or entospletinib
668 (bottom). Scale bar = 10 μm. (B) Quantification of the effects of entospletinib on C3bi-
669 coated and IgG-coated bead uptake by RAW 264.7 cells. Shown is the mean phagocytic
670 index (PI) ± SE for RAW cells incubated in 1 μM entospletinib and allowed to take up
671 C3bi-coated (left) or IgG-coated beads (right), normalized to RAW cells incubated in an
672 equivalent volume of DMSO and the same number of beads (shown as PI = 100%). (C)
673 Enumeration of the effect of entospletinib on C3bi-coated and IgG-coated bead uptake
674 by BMDM. Shown is the mean PI ± SE, calculated through the methodology described in
675 (B). (D, E) Entospletinib does not affect the total number of C3bi- and IgG-coated beads
676 bound to (D) RAW 264.7 cells and (E) BMDM. Shown is the total number of beads per
677 Mϕ ± SE after Mϕ were incubated in 1 μM entospletinib and allowed to take up C3bi-
678 coated (left) or IgG-coated beads (right), normalized to Mϕ incubated in an equivalent
679 volume of DMSO and beads. For B-E: n = 3 separate experiments; *$p < 0.05$, **$p < 0.01$
680 (one sample t-test).

681

682 **Fig. 2. The SYK inhibitor entospletinib decreases *Leishmania* uptake**. Mϕ were
683 treated with entospletinib or DMSO for 2 h and incubated with C3bi-coated *L.*

684 *amazonensis* promastigotes or IgG-coated *L. amazonensis* amastigotes for 30 m.
685 Immunofluorescence was used to distinguish between extracellular (red) and intracellular
686 (green) promastigotes or amastigotes. Mϕ nuclei are labeled with Hoescht 33258. (A)
687 Image of anti-P8 IgG-opsonized amastigote uptake by RAW 264.7 cells treated with
688 DMSO (top) or entospletinib (bottom). Scale bar = 5 μm. (B) Quantification of the effects
689 of entospletinib on promastigote or amastigote uptake by (B) RAW 264.7 cells and (C)
690 BMDM. Shown is the PI ± SE for Mϕ incubated in 1 μM entospletinib and allowed to take
691 up promastigotes (left) or amastigotes (right), normalized to Mϕ incubated in an equivalent
692 volume of DMSO and the same number of beads. (D, E) Entospletinib does not affect the
693 total number of promastigotes and amastigotes bound to (D) RAW 264.7 cells and (E)
694 BMDM. Shown is the total number of parasites per Mϕ ± SE after Mϕ were incubated in 1
695 μM entospletinib and allowed to take up promastigotes (left) or amastigotes (right),
696 normalized to Mϕ incubated in an equivalent volume of DMSO and the same number of
697 parasites. n = 3 separate experiments; $*p < 0.05$, $**p < 0.01$ (one sample t-test).
698
699 **Fig. 3. BMDM lacking SYK exhibit defects in C3bi- and IgG-mediated phagocytosis**
700 **and *L. amazonensis* uptake.** (A) Merged image of promastigote uptake by WT BMDM
701 (top) or *Syk*$^{flox/flox}$ LysM Cre+ BMDM (*Syk*$^{-/-}$ BMDM, bottom), using the methodology
702 described in Fig 2. Scale bar = 10 μm. (B) *Syk*$^{-/-}$ BMDM exhibit defects in promastigote
703 and amastigote uptake. BMDM were incubated with *L. amazonensis* promastigotes or
704 amastigotes as in Fig 2. Graph shows the mean PI ± SE for promastigotes and
705 amastigotes for *Syk*$^{-/-}$ BMDM, normalized to WT BMDM, using the methodology
706 described in Fig 2. (C) Mean normalized total number of promastigotes or amastigotes

707 bound to *Syk*$^{-/-}$ BMDM, normalized to WT BMDM, ± SE. (D) *Syk*$^{-/-}$ BMDM are less able
708 to undergo C3bi and IgG-mediated phagocytosis. BMDM were incubated with C3bi or
709 IgG-coated beads as in Fig 1. Shown is the mean PI ± SE for beads taken up by *Syk*$^{-/-}$
710 BMDM, normalized to WT BMDM (using the methodology described in Fig 1). (E) Mean
711 normalized total number of C3bi or IgG-coated beads bound to *Syk*$^{-/-}$ BMDM, normalized
712 to WT BMDM, ± SE. n = 3 separate experiments; *p<0.05, **p<0.01 (one sample t-test).
713
714 **Fig. 4. A SFK-Abl/Arg-SYK signaling pathway facilitates *Leishmania* uptake.** (A)
715 Treating *Syk*$^{-/-}$ BMDM with SU6656 or imatinib does not further diminish *Leishmania*
716 promastigote (left) or amastigote uptake (right). (B) Entospletinib has no effect on
717 promastigote uptake by BMDM lacking Abl (left) or amastigote uptake by BMDM lacking
718 Hck, Fgr, and Lyn or Arg kinases (right). (C) The Arg/Abl activator DPH does not rescue
719 *Leishmania* promastigote (left) or amastigote uptake (right) in *Syk*$^{-/-}$ BMDM. For all
720 categories, BMDM of the genotypes shown were incubated with DMSO, SU6656,
721 imatinib, entospletinib, or DPH as indicated and allowed to take up promastigotes or
722 amastigotes. PIs were calculated and values were normalized to WT, DMSO treated
723 BMDM (100%). Mean ± SE shown. n = 3 separate biological experiments; *p<0.05,
724 **p<0.01 by ANOVA compared to WT DMSO treated Mϕ.
725
726 **Fig. 5. SYK is activated by SFK/Arg and phosphorylates downstream effectors**
727 **during amastigote uptake.** (A, B) SYK phosphorylation is decreased by inhibition of SFK
728 or Abl family kinases and increased by activating Abl family kinases. RAW 264.7 cells
729 treated with DMSO or inhibitors were incubated with IgG-coated amastigotes (*i.e.*, +

730 amastigotes) for 15 m before processing for immunoblotting. (A) Representative
731 immunoblot of pSYK (top) and total SYK (middle) in DMSO-treated RAW 264.7 cells (±
732 amastigotes) and amastigote-stimulated SU6656, imatinib, entospletinib, or DPH-treated
733 RAW 264.7 cells. GAPDH (bottom) is used as an additional loading control. (B) Graph
734 presents relative pSYK levels, normalized to SYK levels, among RAW 264.7 cell
735 categories shown in (A). pSYK/SYK levels for Mϕs only (*i.e.*, no amastigotes) were
736 normalized to 1. (C, D) Phosphorylation of the SFK/Abl/Arg substrate CrkII (pCrk) induced
737 upon amastigote uptake is decreased in entospletinib-treated Mϕs. (C) Representative
738 immunoblot of pCrk (top) and total CrkII (middle) in DMSO-treated RAW 264.7 cells (±
739 amastigotes) and amastigote-stimulated SU6656, imatinib, entospletinib, or DPH-treated
740 RAW 264.7 cells. GAPDH is used as an additional loading control. (D) Relative levels for
741 pCrk, normalized to CrkII, graphed as in B. n = 3 separate biological experiments; mean
742 ± standard deviations shown. *$p < 0.05$, **$p < 0.01$ by ANOVA compared to pSYK or pCrk
743 levels in WT DMSO-treated Mϕ incubated with amastigotes.
744
745 **Fig. 6. SYK facilitates efficient infection in a mouse model of cutaneous**
746 **leishmaniasis.** (A) Comparison of lesion size in WT versus *Syk*$^{flox/flox}$ LysM Cre+ mice.
747 10 mice per category were infected in the right hind foot with 1 X 10^6 *L. amazonensis*
748 metacyclic promastigotes and monitored over time. Three experiments were performed;
749 shown is a representative experiment. Graphed are the mean ± SE increase in infected
750 foot width when compared to the uninfected foot. *$p < 0.05$ by ANOVA compared to WT
751 mice. (B) *Syk*$^{flox/flox}$ LysM Cre+ mice have a lower parasite burden than WT mice. Plotted
752 is the mean number of parasites isolated from lesions in millions at the termination of (A),

753 ± SE. *$p < 0.05$ by *t*-test. (C) Comparison of lesion size in DMSO vs. entospletinib-treated
754 mice. Experiment performed as in (A), except that mice were treated with 100 mg/kg/d of
755 entospletinib in their drinking water or the equivalent volume of diluent, starting 4 days
756 prior to infection and continuing throughout the experiment. *$p < 0.05$ by ANOVA
757 compared to DMSO-treated mice. (D) Entospletinib-treated mice have a lower parasite
758 burden than DMSO-treated mice. Shown is the mean number of *L. amazonensis*
759 parasites in millions isolated from infected footpads at the termination of (C), calculated
760 as in (B), ± SE. *$p < 0.05$ by *t*-test. (E) Relationship between FcR signaling, SFKs, Arg,
761 and SYK during *Leishmania* amastigote uptake. Upon FcRγ ligation by amastigotes, host
762 cell Hck, Fgr, and Lyn are activated. These SFKs phosphorylate and activate Arg kinase,
763 which phosphorylates and activates SYK. SYK activates other kinases within the host cell
764 (*e.g.,* CrkII), leading to actin polymerization and parasite uptake.
765
766 **Table 1. Cytokine secretion in WT vs *Syk$^{flox/flox}$* LysM Cre+ mice** (abbreviated in the
767 table as *Syk$^{-/-}$*). In general, cytokine secretion after *Leishmania* antigen stimulation is not
768 significantly affected in *Syk$^{flox/flox}$* LysM Cre+ mice. The exception is secretion of IL1-β,
769 for which SYK activity is known to be required. Shown are mean ± SE of cytokine profiles
770 of draining lymph nodes isolated from the WT versus *Syk$^{flox/flox}$* LysM Cre+ mice at the
771 end of the experiment shown in Fig 6, with *p* values calculated by Student's *t*-test. 5 x
772 10^6 cells were cultured for 72 h in medium alone (unstimulated), or with the addition of
773 lysates made from 2.5 x 10^6 (high stimulation) or from 5 x 10^5 (low stimulation) *L.*
774 *amazonensis* parasites. Concanamycin A (Con A) was used as a positive control for

775 stimulation. Media was harvested and used in ELISAs for the above-listed cytokines as
776 described previously (Wetzel *et al.*, 2012; Wetzel *et al.*, 2016).
777
778 **Table 2. Culturing draining lymph nodes with entospletinib does not affect cytokine**
779 **secretion.** Isolated draining lymph nodes from 4 infected DMSO-treated mice were
780 cultured as described as in Table 1, except that either DMSO or 2 μM entospletinib was
781 added to each of these 4 isolated draining lymph nodes during culture for 72 h. Cytokine
782 ELISAs were performed on harvested supernatants as in Table 1. Mean ± SE shown,
783 with *p* values calculated by Students *t*-test. The lone statistically significant result (IL-13,
784 high stimulation) is the opposite of the result that would be expected if immunological
785 effects facilitated healing in entospletinib-treated mice (Jones *et al.*, 1998).
786
787 **Fig. S1. Titrations of entospletinib dosage and effects over time.** (A) Titration of
788 entospletinib's effects on IgG-coated bead uptake by RAW 264.7 cells. Mϕs were treated
789 with DMSO (shown as 0.0 μM entospletinib) or increasing concentrations of entospletinib
790 for 2 h and incubated with IgG-coated beads for 30 m. Shown is one representative
791 experiment of 2 experiments. Data normalized to DMSO category (PI = 100%). (B)
792 Titration of entospletinib's effects on amastigote uptake by RAW 264.7 cells. Mϕs were
793 treated with increasing concentrations of entospletinib or DMSO for 2 h and incubated
794 with IgG-coated amastigotes for 30 m. Shown is one representative experiment of 2
795 experiments. (C) The relative decrease in PI in entospletinib-treated RAW 264.7 cells
796 does not change after long drug incubations. Mϕs were treated with 1 μM entospletinib or
797 DMSO for 2 h and incubated with IgG-coated amastigotes for 30, 60, 120, or 180 m. Data

798 normalized to DMSO, 30 m category. Shown is one representative experiment of 2
799 experiments. (D) Entospletinib log concentration-response curves for RAW 264.7 cells
800 (black) and axenic *L. amazonensis* amastigotes (grey) for one representative experiment
801 of 3 biological replicate experiments. Triplicate technical replicates were used. Cells were
802 incubated for 72 h in the concentrations of entospletinib shown. (E) Treatment with 0.5
803 μM entospletinib has no effects on *L. amazonensis* amastigote survival inside RAW 264.7
804 cells. Mϕs were allowed to internalize *L. amazonensis* amastigotes expressing
805 mNeonGreen, and then, after 24 h, they were incubated with DMSO or 0.5 μM
806 entospletinib for 72 h. Shown is the mean number of *L. amazonensis* amastigotes per
807 100 entospletinib-treated Mϕ, normalized to DMSO-treated Mϕ (100%), ± SE. n = 3
808 separate biological replicates.
809
810 **Table S1. Cytokine secretion is not skewed towards a Th1 or Th2 response during**
811 ***L. amazonensis* infection of *Syk*$^{-/-}$ mice compared to WT mice.** Ratios of IFNγ:IL-4,
812 IFNγ:IL-10, IFNγ:IL-13, and IFNγ:IL-4+10+13 were calculated from the data shown in
813 Table 1.
814

815 **Table 1**

Cytokine	Genotype	Cytokine secretion (pg) after		
		High stimulation	**Low stimulation**	**Con A stimulation**
IL-1β	WT	1,226 ± 91	864 ± 86	1,160 ± 132
	Syk$^{-/-}$	604 ± 55	735 ± 51	750 ± 55
	p	0.000039	0.19	0.0068
IFN-γ	WT	13,044 ± 3,307	9,950 ± 1,344	16,295 ± 3,659
	Syk$^{-/-}$	16,006 ± 3,383	12,084 ± 2,146	14,059 ± 2,088
	p	0.56	0.45	0.59
IL-4	WT	1,094 ± 146	1,093 ± 213	1,168 ± 97
	Syk$^{-/-}$	1,485 ± 240	1,237 ± 172	1,631 ± 364
	p	0.20	0.60	0.30
IL-10	WT	973 ± 292	1,666 ± 516	1,285 ± 433
	Syk$^{-/-}$	1,547 ± 428	990 ± 241	2,091 ± 656
	p	0.30	0.22	0.35
IL-13	WT	824 ± 262	475 ± 104	396 ± 76
	Syk$^{-/-}$	596 ± 119	498 ± 75	616 ± 84
	p	0.41	0.85	0.075
IL-17	WT	< 156	< 156	< 156
	Syk$^{-/-}$	< 156	< 156	< 156
TNF-α	WT	< 124	< 124	< 124
	Syk$^{-/-}$	< 124	< 124	< 124

816

817 **Table 1. Cytokine secretion in WT vs *Syk*$^{flox/flox}$ LysM Cre+ mice** (abbreviated in the

818 table as *Syk*$^{-/-}$).

819

820 **Table 2**

Cytokine	Treatment	Cytokine secretion (pg)	
		High stimulation	**Low stimulation**
IFN-γ	DMSO	10,274 ± 509	13,455 ± 3,689
	Entospletinib	14,140 ± 4,374	19,226 ± 5,478
	p	n.s.	n.s.
IL-4	DMSO	1,522 ± 239	1,183 ± 511
	Entospletinib	1,047 ± 222	832 ± 187
	p	n.s.	n.s.
IL-10	DMSO	1,631 ± 442	2,013 ± 820
	Entospletinib	2,664 ± 424	2,451 ± 657
	p	n.s.	n.s.
IL-13	DMSO	342 ± 34.5	330 ± 36.6
	Entospletinib	491 ± 20.3	452 ± 53.2
	p	0.021	n.s.

821

822 **Table 2. Culturing draining lymph nodes with entospletinib does not affect cytokine**

823 **secretion.**

Figure 1

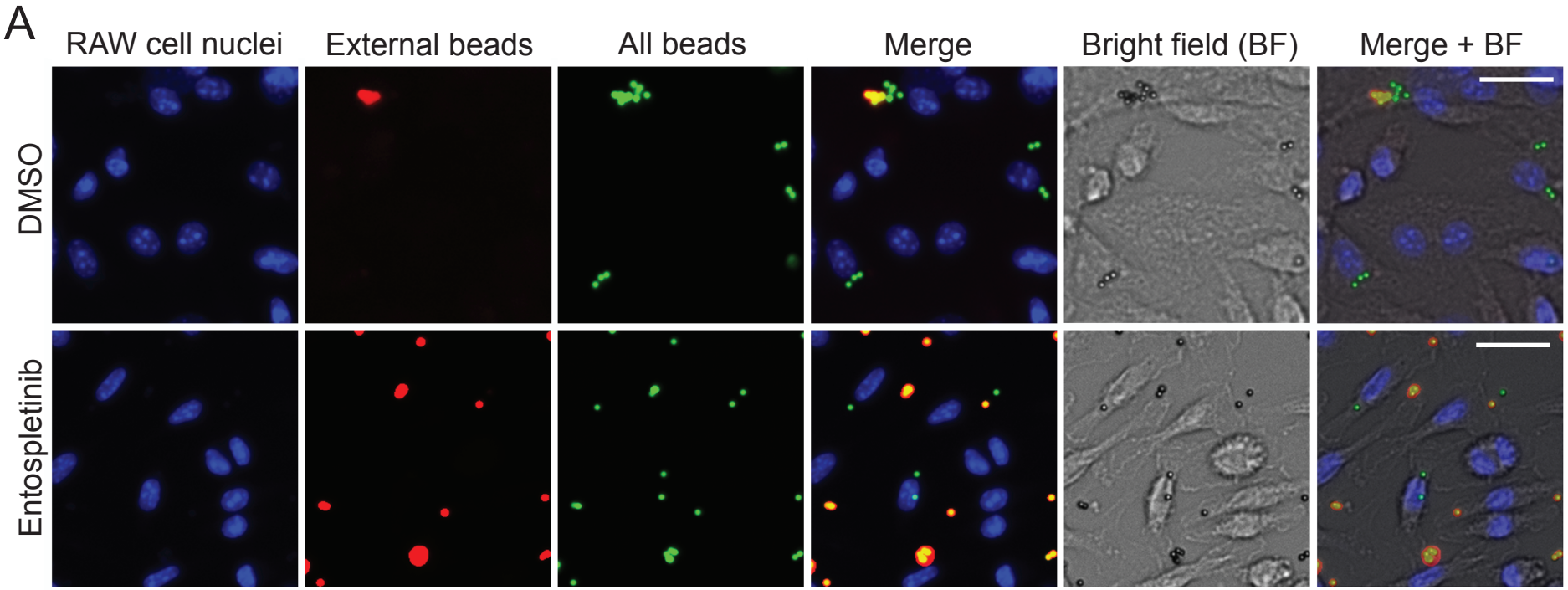
A
RAW cell nuclei
External beads
All beads
Merge
Bright field (BF)
Merge + BF
DMSO
Entospletinib

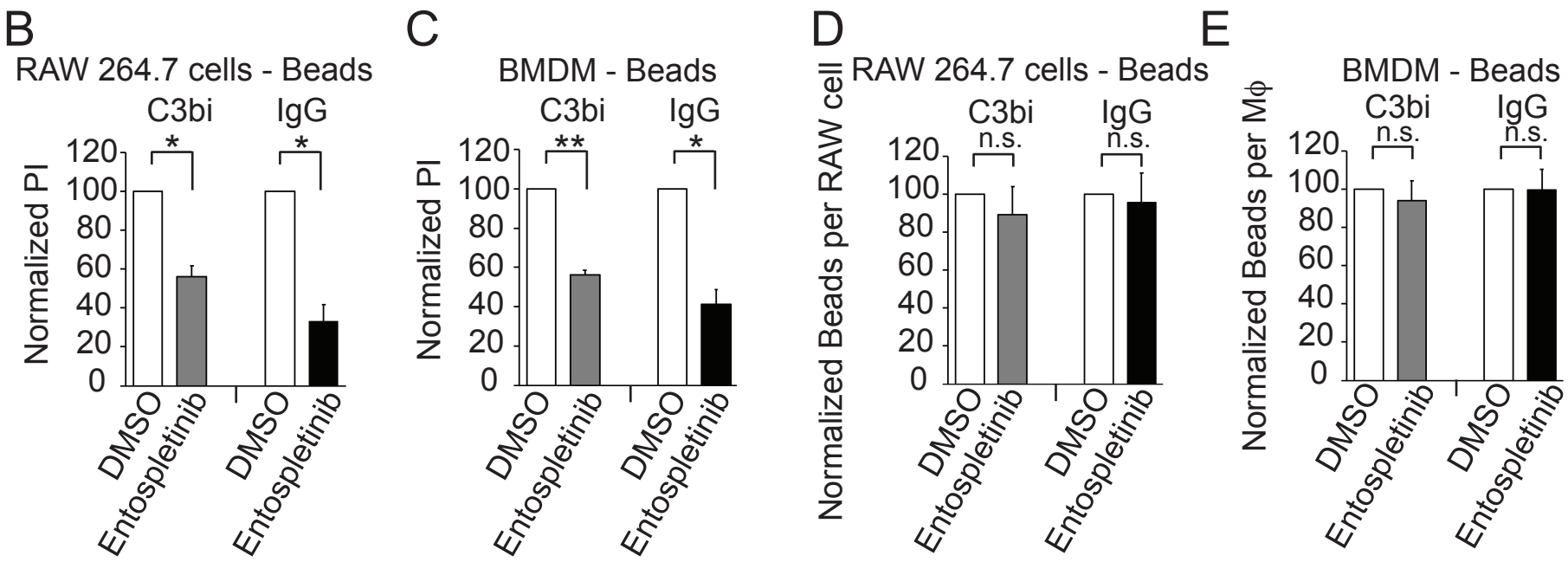
B
RAW 264.7 cells - Beads
C3bi
IgG
Normalized PI
120
100
80
60
40
20
0
*
*
DMSO
Entospletinib
DMSO
Entospletinib
C
BMDM - Beads
C3bi
IgG
Normalized PI
**
*
D
RAW 264.7 cells - Beads
Normalized Beads per RAW cell
n.s.
n.s.
E
BMDM - Beads
Normalized Beads per Mϕ
n.s.
n.s.

Figure 2

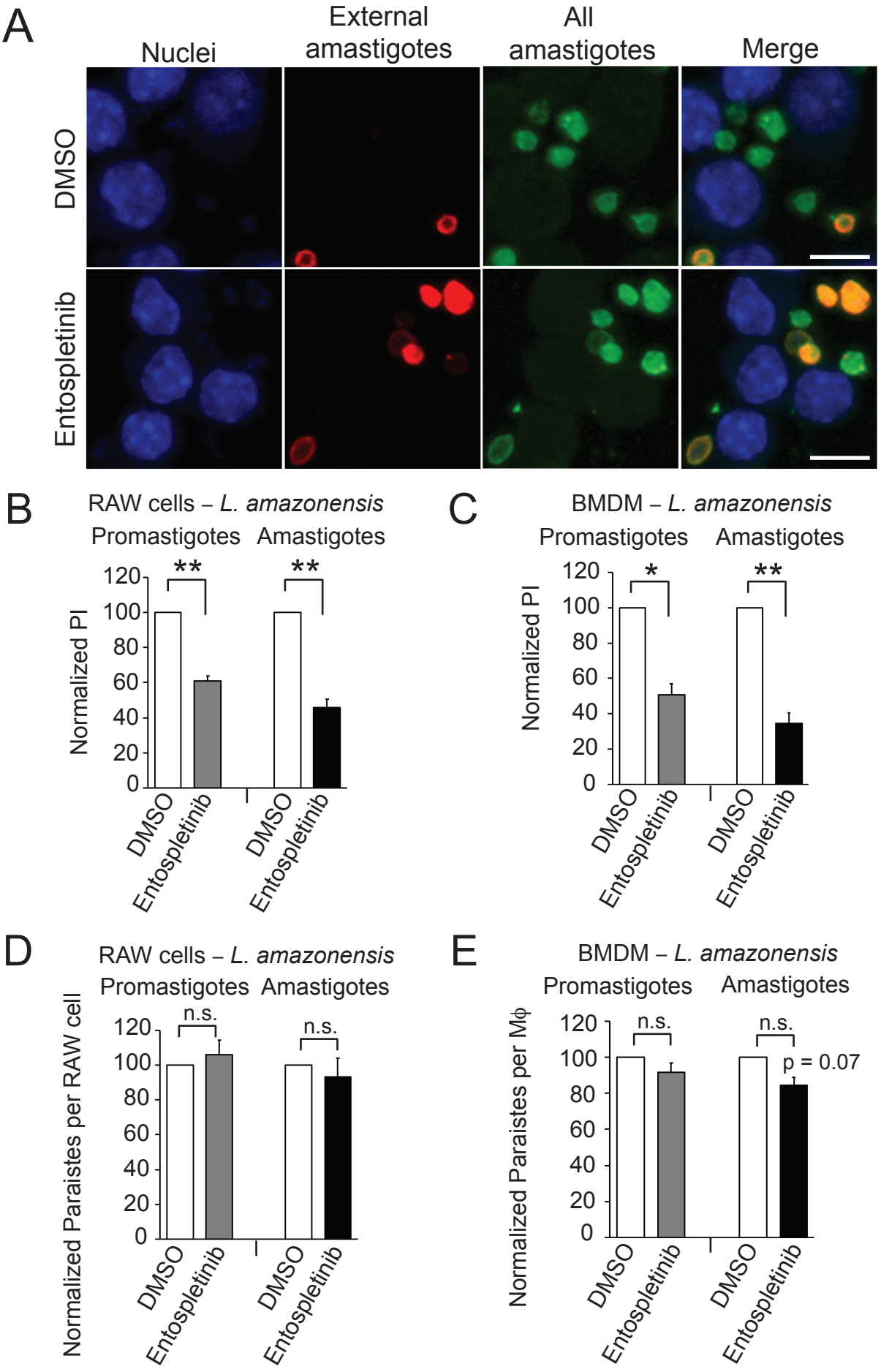
A
Nuclei
External amastigotes
All amastigotes
Merge
DMSO
Entospletinib
B
RAW cells – L. amazonensis
Promastigotes
Amastigotes
Normalized PI
120
100
80
60
40
20
0
**
**
DMSO
Entospletinib
DMSO
Entospletinib
C
BMDM – L. amazonensis
Promastigotes
Amastigotes
Normalized PI
*
**
DMSO
Entospletinib
DMSO
Entospletinib
D
RAW cells – L. amazonensis
Promastigotes
Amastigotes
Normalized Paraistes per RAW cell
n.s.
n.s.
DMSO
Entospletinib
DMSO
Entospletinib
E
BMDM – L. amazonensis
Promastigotes
Amastigotes
Normalized Paraistes per Mϕ
n.s.
n.s.
p = 0.07
DMSO
Entospletinib
DMSO
Entospletinib

Figure 3

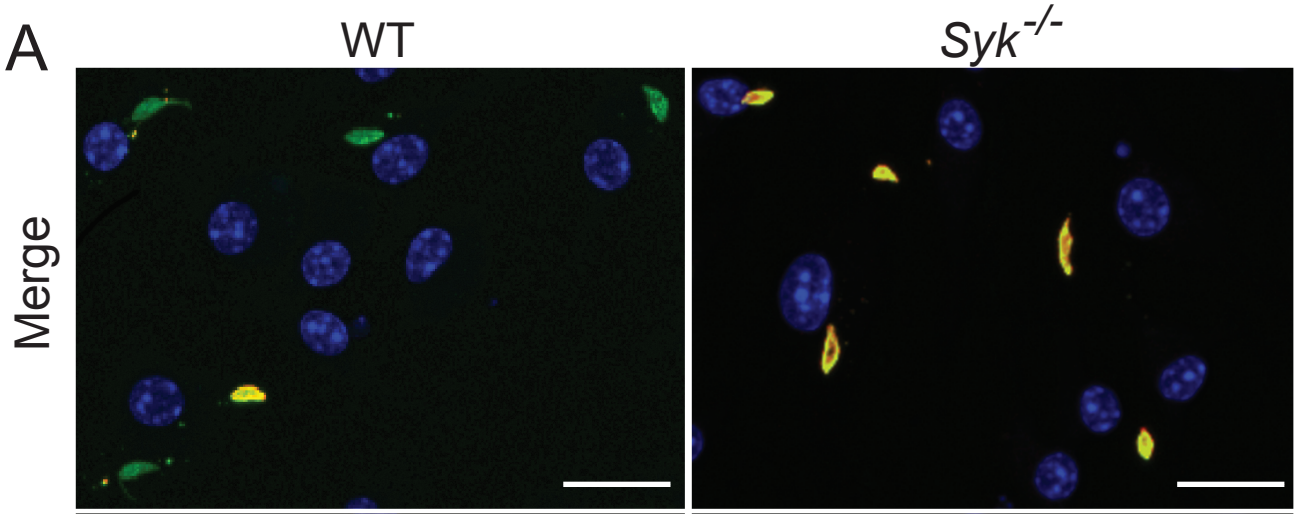
A
WT
Syk-/-
Merge

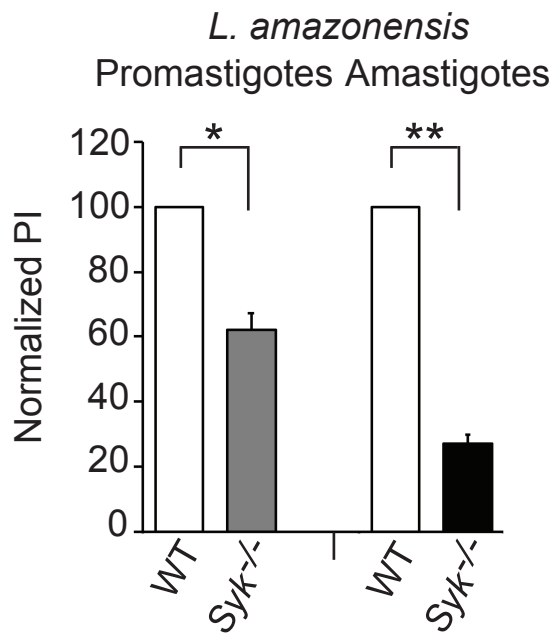
B
L. amazonensis
Promastigotes Amastigotes
Normalized PI
120
100
80
60
40
20
0
*
**
WT
Syk-/-
WT
Syk-/-

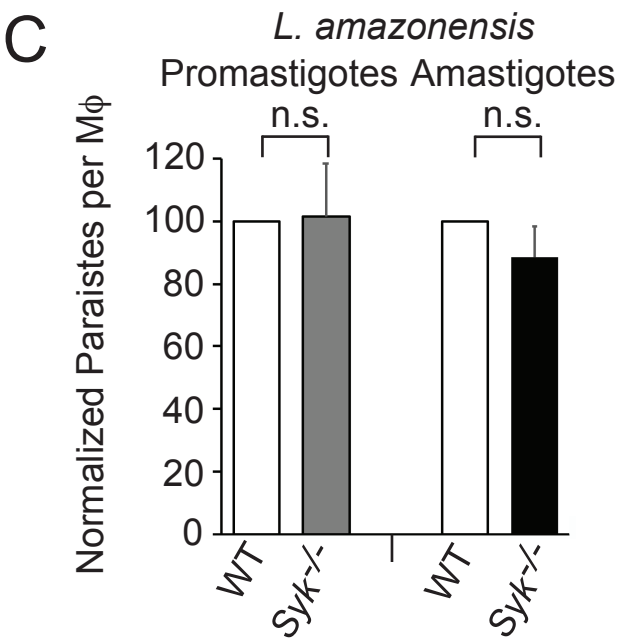
C
L. amazonensis
Promastigotes Amastigotes
n.s.
n.s.
Normalized Paraistes per Mϕ
120
100
80
60
40
20
0
WT
Syk-/-
WT
Syk-/-

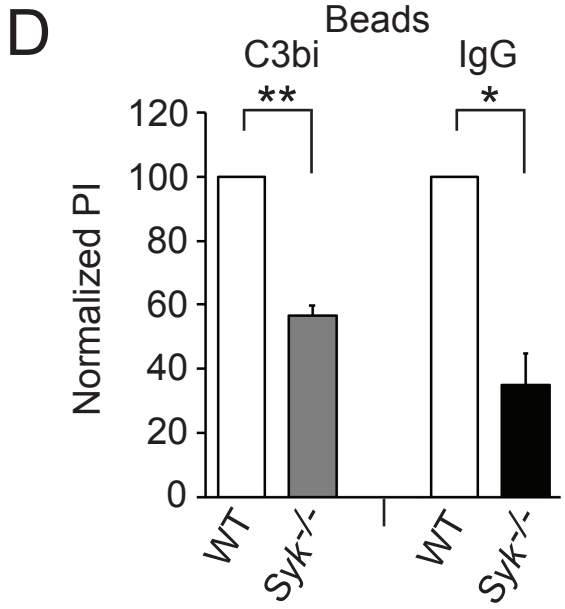
D
Beads
C3bi
IgG
**
*
Normalized PI
120
100
80
60
40
20
0
WT
Syk-/-
WT
Syk-/-

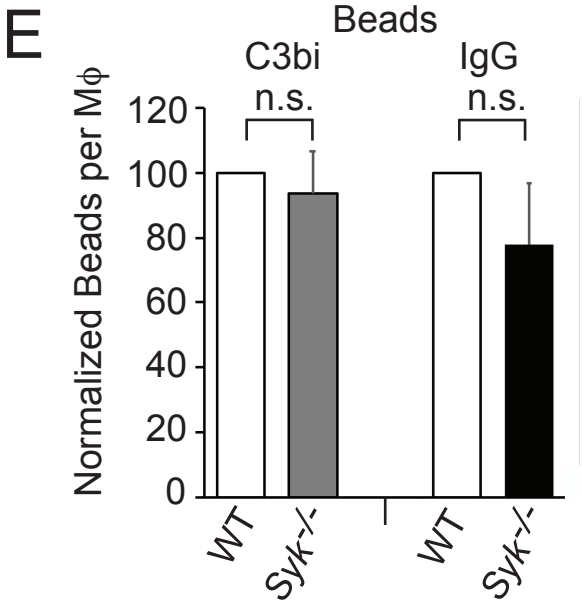
E
Beads
C3bi
IgG
n.s.
n.s.
Normalized Beads per Mϕ
120
100
80
60
40
20
0
WT
Syk-/-
WT
Syk-/-

Figure 4

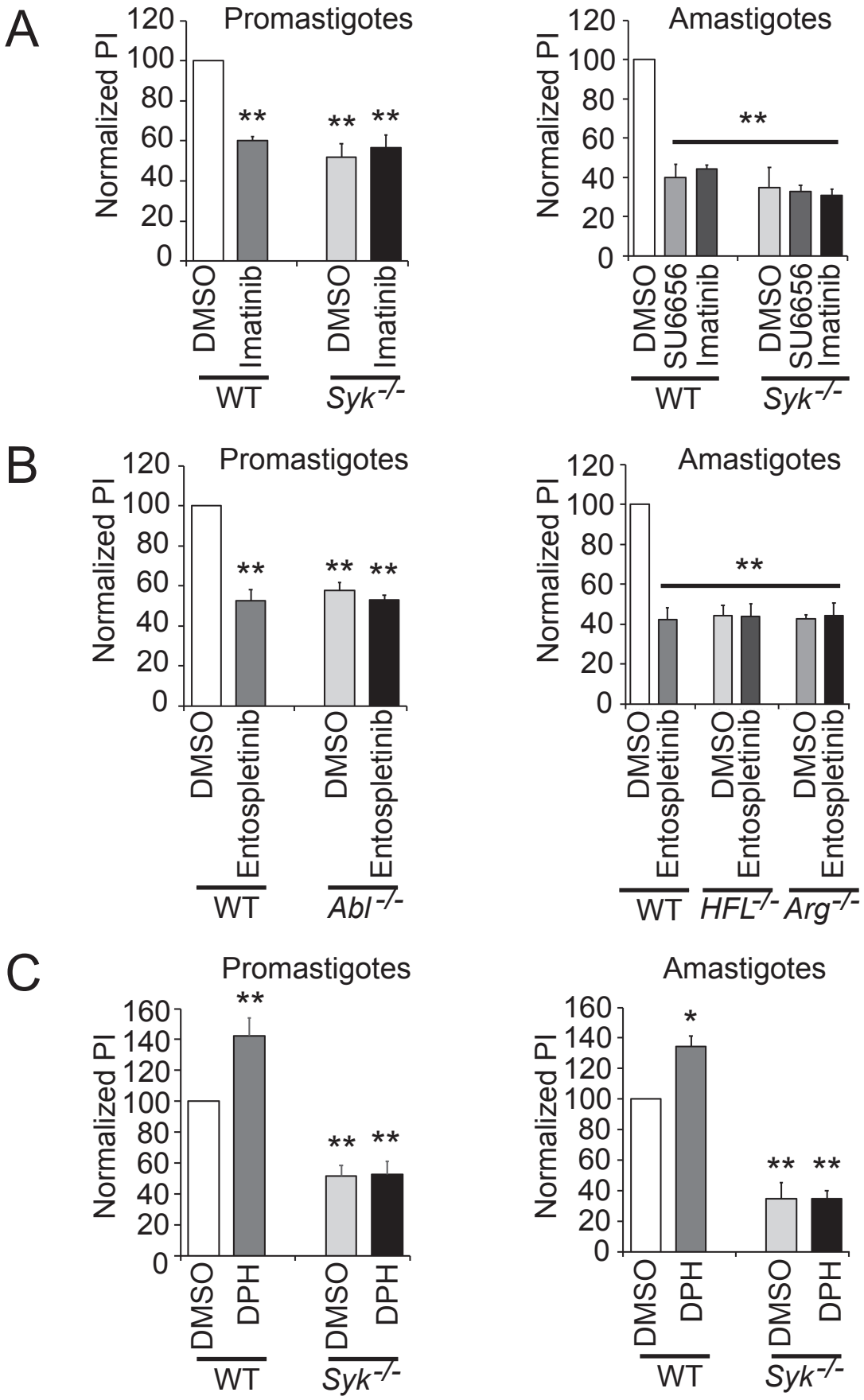
A
Promastigotes
Amastigotes
Normalized PI
120
100
80
60
40
20
0
**
DMSO
Imatinib
SU6656
WT
Syk-/-
B
Entospletinib
Abl-/-
HFL-/-
Arg-/-
C
DPH
*

Figure 5

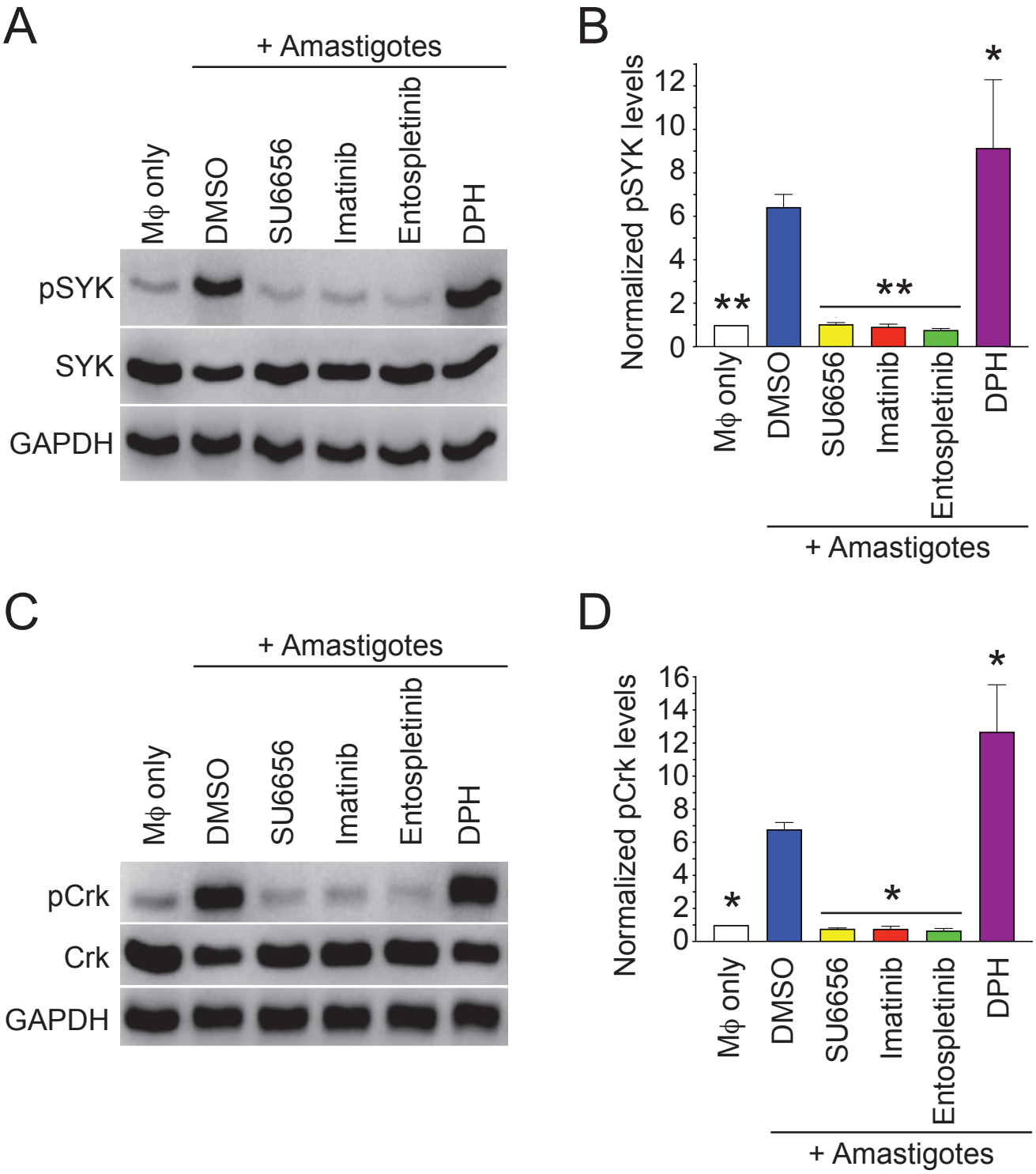
A
+ Amastigotes
Mϕ only
DMSO
SU6656
Imatinib
Entospletinib
DPH
pSYK
SYK
GAPDH
B
Normalized pSYK levels
0
2
4
6
8
10
12
**
**
*
Mϕ only
DMSO
SU6656
Imatinib
Entospletinib
DPH
+ Amastigotes
C
+ Amastigotes
Mϕ only
DMSO
SU6656
Imatinib
Entospletinib
DPH
pCrk
Crk
GAPDH
D
Normalized pCrk levels
0
2
4
6
8
10
12
14
16
*
*
*
Mϕ only
DMSO
SU6656
Imatinib
Entospletinib
DPH
+ Amastigotes

Figure 6

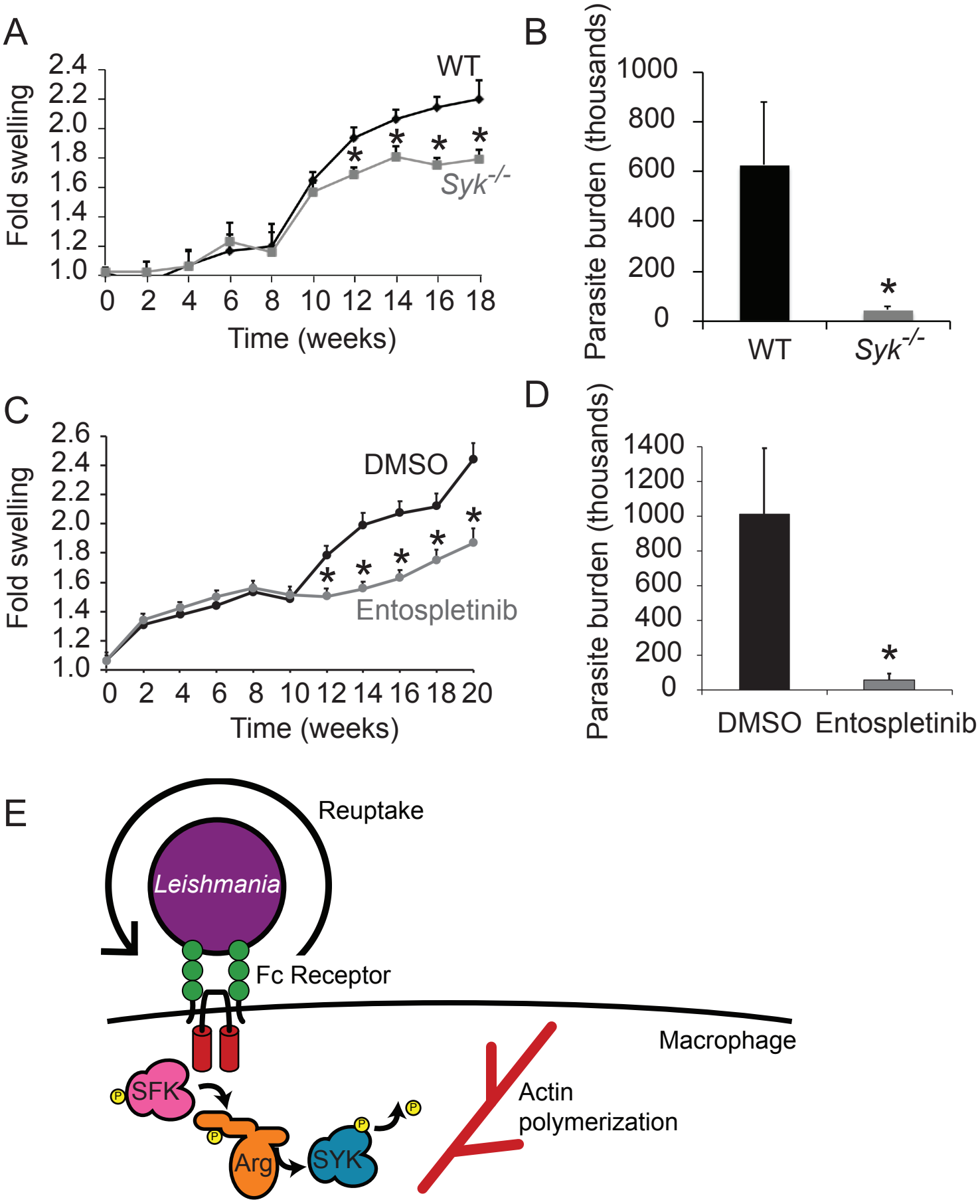
A
Fold swelling
2.4
2.2
2.0
1.8
1.6
1.4
1.2
1.0
WT
Syk-/-
0 2 4 6 8 10 12 14 16 18
Time (weeks)
B
Parasite burden (thousands)
1000
800
600
400
200
0
WT
Syk-/-
C
Fold swelling
2.6
2.4
2.2
2.0
1.8
1.6
1.4
1.2
1.0
DMSO
Entospletinib
0 2 4 6 8 10 12 14 16 18 20
Time (weeks)
D
Parasite burden (thousands)
1400
1200
1000
800
600
400
200
0
DMSO
Entospletinib
E
Reuptake
Leishmania
Fc Receptor
Macrophage
SFK
Arg
SYK
Actin
polymerization